THE JOURNAL OF BIOLOGICAL CHEMISTRY VOL. 281, NO. 51, pp. 39699–39707, December 22, 2006

Identification of a Mutation in SLC30A2 (ZnT-2) in Women with Low Milk Zinc Concentration That Results in Transient Neonatal Zinc Deficiency*

Received for publication, June 19, 2006, and in revised form, October 5, 2006 Published, JBC Papers in Press, October 25, 2006, DOI 10.1074/jbc.M605821200

Winyoo Chowanadisai, Bo Lönnerdal, and Shannon L. Kelleher[1]

From the Department of Nutrition, University of California, Davis, California 95616

Breast milk normally contains adequate zinc to meet infant requirements up to six months of age; however, transient neonatal zinc deficiency has been documented in exclusively breast-fed infants of women with low milk zinc concentration. This condition is not corrected by maternal zinc supplementation, supporting the speculation that it results from an inherited genetic condition. We identified a family in which two exclusively breast-fed infants developed zinc deficiency that was associated with low milk zinc concentration in both women. Sequencing of genomic DNA detected a mis-sense mutation (Ade→Gua) that substitutes a conserved histidine at amino acid 54 with arginine (H54R) in SLC30A2 (ZnT-2) that is present in both affected subjects and several other siblings. Gene knockdown of SLC30A2 in mammary epithelial cells reduced zinc secretion, illustrating the role of ZnT-2 in zinc secretion from this cell type. Expression of the H54R mutant in human embryonic kidney-293 cells resulted in reduced zinc secretion as a consequence of perinuclear, aggresomal accumulation, whereas co-expression of the H54R mutant and wild-type ZnT-2 did not abrogate increased zinc secretion in cells overexpressing wild-type ZnT-2 alone. Together, these data provide evidence that low milk zinc concentration in some women is a consequence of a genetic disorder resulting from a mutation in SLC30A2 and can result in neonatal zinc deficiency if unrecognized. Further studies are needed to evaluate the incidence and penetrance of this mutation in the human population.

Zinc is an essential trace mineral and zinc deficiency can lead to dermatitis, alopecia, decreased growth, and impaired immune function (1). Infants are particularly vulnerable because of the large amount of zinc required for growth during this period. Breast milk normally contains adequate zinc to meet the requirement for infants up to 4–6 months of age (2); however, numerous reports have documented transient or acquired neonatal zinc deficiency in breast-fed infants (3–7) as a consequence of low milk zinc concentration in their nursing mothers, which cannot be corrected by maternal zinc supplementation (4, 5). Although the etiology of this disorder is unknown, it is presumably the result of an inherited genetic condition (zinc in breast milk, reduced; OMIM 608118) and elegantly highlights the interplay between genetics and nutrition. Transient neonatal zinc deficiency resembles some aspects of two previously identified genetic defects in mammalian zinc metabolism, acrodermatitis enteropathica (AE[2]; Online Mendelian Inheritance in Man (OMIM) 201100) in humans and the lethal milk mutation (*lm/lm*; OMIM 602095) in mice. Acrodermatitis enteropathica is a rare, autosomal recessive disorder that results in severe zinc deficiency as a consequence of impaired intestinal zinc absorption (8) due to mutations in SLC39A4, which encodes the zinc importer Zip4 (9, 10). Lethal milk mice (lm^{-}/lm^{-}) have a mutation in SLC30A4 resulting in early translational termination and truncation of the zinc transporter ZnT-4 (11), which is associated with reduced milk zinc concentration and neonatal zinc deficiency in pups nursed from afflicted dams (12). However, transient neonatal zinc deficiency in humans is different from both conditions. Unlike infants with AE, zinc absorption in infants with transient neonatal zinc deficiency is normal (3), and symptomatic zinc deficiency only exists during exclusive nursing, suggesting the genetic defect and corresponding phenotype is maternal in presentation. Thus, infants with transient neonatal zinc deficiency do not require zinc supplementation following weaning, whereas AE patients require lifelong zinc supplementation. Unfortunately, transient neonatal zinc deficiency is often misdiagnosed as AE, which can have severe health implications as zinc oversupplementation can induce copper deficiency and immune dysfunction (13), further highlighting the importance of adequately diagnosing and treating this disorder as early as possible. Transient neonatal zinc deficiency in humans is also clinically distinct from symptoms in lm^{-}/lm^{-} mice in that no maternal symptoms, other than low breast milk zinc concentration, have been reported in affected humans, whereas lm^{-}/lm^{-} mice develop zinc deficiency with age (14) and lack utricular otoconia, resulting in abnormalities in the balance system (14). Moreover, no mutations in SLC30A4 were found in two affected individuals by Michalczyk *et al.* (7), suggesting that the human homologue of SLC30A4 is not affected in mothers of infants with transient neonatal zinc deficiency.

Consequently, we speculate that transient neonatal zinc deficiency in humans is unique from these two previously reported genetic disorders in mammalian zinc metabolism and results

* The costs of publication of this article were defrayed in part by the payment of page charges. This article must therefore be hereby marked "*advertisement*" in accordance with 18 U.S.C. Section 1734 solely to indicate this fact.

[1] To whom correspondence should be addressed: Dept. of Nutrition, University of California, One Shields Ave., Davis, CA 95616. Tel.: 530-754-4414; Fax: 530-752-8966; E-mail: slkelleher@ucdavis.edu.

[2] The abbreviations used are: AE, acrodermatitis enteropathica; HA, hemagglutinin; siRNA, small interfering RNA; HEK, human embryonic kidney; PBS, phosphate-buffered saline.

from a mutation in another zinc transporter with yet undefined function. Toward this end, we have previously documented SLC30A2 (ZnT-2) and SLC39A3 (Zip3) expression in the mammary gland of lactating rats and determined that changes in ZnT-2 and Zip3 protein abundance parallel changes in milk zinc concentration (15). Furthermore, we have characterized the reliance upon Zip3 for zinc uptake in mammary epithelial cells, which taken together suggests that these genes represent likely candidates for the defective allele. We therefore hypothesized that a mutation in one of these two genes is responsible for low breast milk zinc concentration in humans leading to transient neonatal zinc deficiency. Herein, we identified a missense mutation in SLC30A2 in affected members of a family with low milk zinc concentration and demonstrated that the mutation results in perinuclear, aggresomal accumulation of the mutated form of ZnT-2 and reduced zinc secretion from transfected human embryonic kidney (HEK)-293 cells, indicating that a mutation in SLC30A2 may be responsible for at least some cases of transient neonatal zinc deficiency in humans.

EXPERIMENTAL PROCEDURES

Clinical Data of Subjects—Written consent was obtained from all subjects, and the study was approved by the University of California, Davis, Institutional Review Board. Serum and milk zinc concentration was determined by independent laboratory testing and obtained from patient medical records. Zinc deficiency was diagnosed by the infants' doctors based upon clinical symptoms and confirmed by serum zinc concentration when possible. Retrospective infant dietary and treatment records were obtained by questionnaire from each infant's mother. Dietary questions included length of breast-feeding, whether infant diet included formula feeding and how often and when it was initiated, and whether nutritional supplements were given. Infant photos were taken by the mother accompanied by the date the photos were taken and were not retouched.

Sequence Analysis of SLC30A2, SLC39A3, and SLC30A4—Genomic DNA was isolated from the whole blood of two women with low milk zinc concentration (Paxgene Blood DNA Kit, Qiagen, Valencia, CA). The coding regions (including splice sites), 5′- and 3′-untranslated regions and at least 1 kb upstream of the first exon of SLC30A2, SLC39A3, and SLC30A4 (to confirm previous reports), were amplified by PCR (Invitrogen Platinum Hi Fidelity *Taq* and Clontech GC genomic polymerase, BD Biosciences). PCR primer information is available upon request. Both splice variants of SLC39A3 were sequenced. PCR products were subcloned into TOPO XL Vector (Invitrogen) and sequenced by the University of California, Davis, Division of Biological Sciences Automated DNA Sequencing Facility (Davis, CA).

Sequence translations and analyses were performed using Bioedit software (16), and sequence chromatograms were visually analyzed for mutations. The Ade→Gua substitution in SLC30A2 was confirmed in each sample with duplicate PCR reactions sequenced in both directions. Sequences for human (NCBI protein identification number NP_115902), rat (NP_037022), and mouse (XP_131731) SLC30A2; human (NP_003450) and mouse (NP_035903) SLC30A3; human (NP_776250) and mouse (NP_766404) SLC30A8; and human (NP_037441), mouse (NP_035904), frog (*Xenopus*, AAH82626), and zebrafish (*Danio*, NP_956937) SLC30A4 were obtained from the National Center for Biotechnology Information (NCBI; www.ncbi.nlm.nih.gov). Amino acid sequences were aligned with ClustalW and Boxshade.

Vector Construction and Site-directed Mutagenesis of SLC30A2—Human SLC30A2 cDNA was obtained from a cDNA clone (accession number CR592804; Invitrogen). The Ade→Gua substitution was introduced by PCR mutagenesis with the primers 5′-GCCCAGAGCAACCATCACTGCC-GTGCTCAGAAGGGTCCTGACAGT-3′ and 5′-ACTGT-CAGGACCCTTCTGAGCACGGCAGTGATGGTTGCTC-TGGGC-3′ (mutation underlined; 25 cycles at 94 °C for 20 s, 60 °C for 30 s, 68 °C for 5 min with Invitrogen Platinum *Pfx* DNA polymerase) followed by digestion of the parental strand by DpnI. The entire coding region and the 5′-untranslated region of the wild-type and mutated forms of human SLC30A2 were amplified and tagged at the C terminus with two tandem hemagglutinin (HA) epitopes by PCR using primers 5′-GAGACACGGGAGCGCTTGGC-3′ and 5′-CATCAGGCGTAGTCGGGGACGTCGTAGGGGTAGG-CGTAGTCGGGGACGTCGTAGGGGTAGTCTGAGGG-GCCCTGGCATGC-3′ (containing epitope tags and a terminal stop codon; 25 cycles: 94 °C for 30 s and 68 °C for 2.5 min) (BD Advantage-GC Genomic PCR; BD Biosystems) and inserted into pcDNA3.1/V5-His TOPO vector (Invitrogen). The site-directed mutation, orientation and fidelity of the insert, and incorporation of the epitope tag were confirmed by directed sequencing (Univeristy of California, Davis, Division of Biological Sciences Automated DNA Sequencing Facility).

Cell Culture and Transient Transfection—Mouse mammary epithelial cells (HC11) abundantly express ZnT-2 and thus were used for transient knockdown of ZnT-2 expression to determine endogenous ZnT-2 function. HC11 cells were a gift from Dr. Jeffery Rosen (Houston, Texas) and used with permission of Dr. Bernd Groner (Institute for Biomedical Research, Frankfurt, Germany). HC11 cells were grown in RPMI 1640 medium supplemented with 10% fetal bovine serum, gentamycin (50 mg/liter; Sigma), insulin (5 mg/liter; Sigma), and epidermal growth factor (10 μg/liter; Sigma) at 37 °C and 5% CO_2. For small interfering RNA (siRNA)-mediated knockdown experiments, HC11 cells were seeded in antibiotic-free growth medium in 24-well plates (2×10^5 cells/well) for zinc uptake and secretion studies and in 6-well plates (4×10^5 cells/well) for verification of reduced ZnT-2 mRNA and protein abundance and cultured overnight until ~50% confluent. The cells were transfected with 50 pmol (24-well plates) or 100 pmol (6-well plates) of either SLC30A2-specific (sense, 5′-CCGAG-CUGCCUUCAUUCAUGUGAUU-3′; antisense, 5′-AAUCA-CAUGAAUGAAGGCAGCUCGG-3′) or mismatch control siRNA (sense, 5′-CCGCGUCCUUCCUUAUGUAGGAAUU-3′; antisense, 5′-AAUUCCUACAUAAGGAAGGACGCGG-3′) (Invitrogen Stealth siRNA) in antibiotic-free growth medium using Lipofectamine 2000 (Invitrogen) at an oligonucleotide:transfection reagent ratio of 25:1 (according to manufacturer's specifications) for 16 h prior to experiments. SLC30A2 knockdown was verified by reduction in ZnT-2 mRNA and protein abundance by real-time reverse transcrip-

tion-PCR and immunoblotting, respectively, and effects on zinc secretion were measured using ^{65}Zn as described below.

HEK-293 cells lack detectable endogenous ZnT-2 expression and thus were used for determining the effects of the H54R mutated form of ZnT-2 on zinc uptake, zinc secretion, and subcellular localization. HEK-293 cells (American Type Culture Collection, Manassas, VA) were grown in Dulbecco's modified Eagle's medium supplemented with 10% fetal bovine serum (Sigma) and penicillin/streptomycin (100 units/liter; Sigma) at 37 °C and 5% CO_2. The cells were seeded in antibiotic-free growth medium in 6-well plates (2.5×10^6 cells/well) for protein abundance or in 24-well plates (6×10^5 cells/well) for zinc secretion, zinc uptake, and subcellular localization studies and cultured overnight until ~95% confluent. The cells were transfected with 1.6 μg (24-well plates) or 8 μg (6-well plates) of empty pcDNA3.1 plasmid or plasmid containing wild-type or H54R mutant SLC30A2 (or equal amounts of wild-type and mutant plasmid) in serum- and antibiotic-free growth medium using Lipofectamine 2000 at a DNA:transfection reagent ratio of 1:2.5 according to the manufacturer's specifications. Transfection medium was replaced 16 h later with antibiotic-free growth medium, and cells were cultured for an additional 24 h prior to experiments.

Indirect Immunofluorescence Microscopy—HEK-293 cells were seeded onto sterile glass coverslips and transfected with plasmid containing wild-type or H54R mutant SLC30A2 fused to HA as described above. After 48 h (post-transfection), the cells were fixed with 4% paraformaldehyde in phosphate-buffered saline (PBS) for 30 min and permeabilized with 0.2% Triton X-100 in PBS for 6 min. Nonspecific binding was blocked with 4% bovine serum albumin in PBS for 30 min, and transfected ZnT-2 protein was detected following incubation with mouse anti-HA antibody conjugated to Alexa 488 (Invitrogen; 1:250 in PBS with 4% bovine serum albumin) for 1 h. Cells were extensively washed, and nuclei were stained with TOPRO Nuclear Stain 647 (1 μM; Invitrogen) for 30 min. No staining was observed when anti-HA antibody was omitted during the staining process (data not shown). Coverslips were mounted in ProLong Gold (Invitrogen) and sealed with nail polish. Immunofluorescent imaging was performed using a Radiance 2100 Confocal System with an argon-red diode laser (Bio-Rad). An Olympus BX50WI microscope with a X100 UPlanApo oil immersion lens was used for visualization. Digital images were captured using LaserSharp2000, version 4.1 (Bio-Rad), and saved as RGB jpeg files to maintain image quality.

Immunoblotting—HEK-293 cells were transfected with the empty pcDNA3.1 plasmid, plasmid containing wild-type or H54R mutant SLC30A2, or β-galactosidase (Clontech, to monitor transfection efficiency) as described above. The cells were scraped into ice-cold lysis buffer (20 mM Hepes, pH 7.4; 1 mM EDTA; 250 mM sucrose) containing protease inhibitors (0.2 mmol/liter 4-(2-aminoethyl)-benzenesulfonyl fluoride, 0.1 mmol/liter EDTA, 13 μmol/liter bestatin, 1.4 μmol/liter ME-64, 0.1 μmol/liter leupeptin, and 0.03 μmol/liter aprotinin; Sigma) and sonicated twice for 10 s on ice. A slow-sedimenting, post-nuclear supernatant was isolated by centrifugation for 5 min at 2000 $\times$ *g* at 4 °C (to pellet nuclei, cell debris, and aggregated protein), and protein concentration in the resulting cell lysate was determined by Bradford assay. Alternatively, a low speed, post-nuclear supernatant was isolated by centrifugation for 5 min at 800 $\times$ *g* at 4 °C (to pellet nuclei and cell debris), and the crude membrane fraction was pelleted at 100,000 $\times$ *g* for 30 min at 4 °C. The resulting crude membrane pellet was resuspended in SDS sample buffer containing dithiothreitol (100 mM). Total cell lysate or crude membrane protein (30 μg/well) was separated by 10% SDS-PAGE under reducing conditions (100 mM dithiothreitol) and transferred to nitrocellulose membrane. Membranes were blocked overnight at 4 °C in 5% nonfat milk in PBST (PBS containing 0.1% Tween 20), incubated with rabbit anti-HA (0.5 μg/ml; Sigma), affinity-purified rabbit anti-ZnT-2 (2 μg/ml), rabbit anti-β-galactosidase (0.4 μg/ml; Invitrogen), or mouse anti-β-actin (1:5000; Sigma) antibodies for 1 h at room temperature and detected with either donkey anti-rabbit or anti-mouse IgG antibody (both conjugated to horseradish peroxidase). The production of the anti-ZnT-2 antibody has been described previously (17). This antibody detects both wild-type and mutant ZnT-2, and the C terminus location of the ZnT-2 sequence containing the immunizing peptide sequence is distinct from the N terminus location of the mutation. Bands were visualized by enhanced chemiluminescence (SuperSignal Femto, Pierce) and quantified by densitometry (Quantity One, Bio-Rad).

Isolation of Aggresomes—Aggresomes were isolated following the detergent insolubility method of Matsumoto *et al.* (18). Briefly, HEK-293 cells transfected with equal quantities of empty plasmid or plasmid containing wild-type or H54R mutant SLC30A2 were washed with PBS, scraped, and harvested by centrifugation. The cells were resuspended in lysis buffer (20 mM Hepes, pH 7.9, containing 25% glycerol, 420 mM NaCl, 1.5 mM $MgCl_2$, 0.2 mM EDTA, and 1 mM phenylmethylsulfonyl fluoride), vortexed, and lysed by the freeze/thaw method. Total protein was measured by Bradford assay, and 100 μg of the protein was diluted with 1 ml of 1% SDS in PBS and then loaded under vacuum onto a cellulose acetate membrane. Membranes were washed with 3 ml of 1% SDS/PBS and slightly vacuum-dried and then immunoblotted using mouse anti-HA antibody (1 μg/ml) as described above.

Zinc Uptake and Secretion—Zinc uptake was measured in transfected cells treated with serum-free RPMI 1640 (HC11 cells; to assess effects of SLC30A2 knockdown) or serum-free Dulbecco's modified Eagle's medium (HEK-293 cells; to assess effects of H54R mutation) containing 2 μM $ZnSO_4$ and 0.1 μCi ^{65}Zn (2.94 mCi/mg, Los Alamos National Laboratory, Los Alamos, NM) for 30 min at 37 °C. The medium was removed and cells were washed three times with ice-cold PBS containing 1 mM EDTA to remove exofacially bound ^{65}Zn, and zinc uptake was measured in cells solubilized with 1 N NaOH. Conversely, cells were loaded with ^{65}Zn diluted into serum-free medium containing 2 μM $ZnSO_4$ and ^{65}Zn (0.1 μCi) for 2.5 h. The medium was removed, and the cells were washed with prewarmed PBS and incubated with prewarmed medium without serum for up to 30 min at 37 °C. The radioactivity in the medium (zinc secretion) was measured in a γ scintillation counter (Packard Minaxi-γ; Meriden, CT).

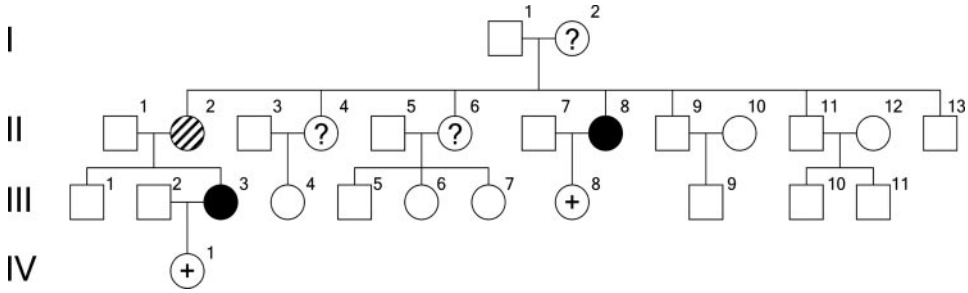

FIGURE 1. **Pedigree of a family afflicted with transient neonatal zinc deficiency. Roman numerals denote generation and Arabic numbers denote family members.** The two phenotypes, confirmed by milk zinc analysis, are indicated by a *filled circle*. A suspected but unconfirmed phenotype is marked with a *hatched circle*. Ambiguous phenotypes, without milk zinc data, are marked with a *question mark*. Infants diagnosed with zinc deficiency are marked with a *plus symbol*.

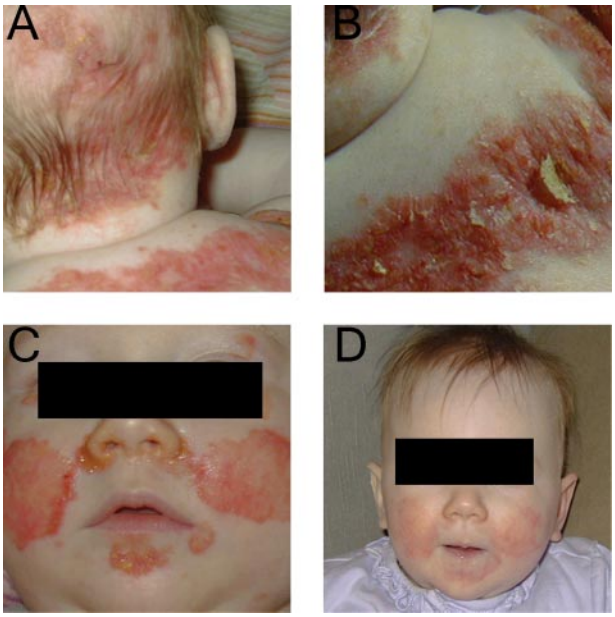

FIGURE 2. **Photographs of an affected infant with transient neonatal zinc deficiency.** Images clearly illustrating severe dermatitis were taken by the mother of individual 111:8 before diagnosis at five months of age (*A–C*) and seven days after zinc supplementation (*D*).

Quantification of SLC30A2 mRNA Levels by Real-time Reverse Transcription-PCR—Total RNA was isolated from HC11 cells using TRIzol (Invitrogen), according to the manufacturer's instructions, and diluted to 1 μg/μl in RNase-free water. cDNA was generated from 1 μg of RNA by reverse transcription (Applied Biosystems, Foster City, CA) performed at 48 °C for 30 min followed by 95 °C for 5 min. Real-time PCR was performed using the cDNA reaction mixture (1.5 μl) using the ABI 7900HT real-time thermocycler (Applied Biosystems) coupled with SYBR Green technology (Applied Biosystems) using gene-specific primers to either mouse SLC30A2 (forward, 5′-GCCCAGGAAGCCAAGTCA-3′; reverse, 5′-GAGAGCAAGA TCTAACTGGAATCTATCA-3′) or GAPDH (forward, 5′-CCACCCCAGCAAGGACACT-3′; reverse, 5′-GAAATTGTGAGGGAGATGCTCAGT-3′). Primers were designed by Primer Express (Applied Biosystems). The PCR cycling parameters were as follows: 50 °C for 2 min, 95 °C for 10 min, 40 cycles of 95 °C for 15 s, 60 °C for 1 min, followed by 95 °C for 15 s. The linearity of the dissociation curve was analyzed by ABI 7900HT software, and the mean cycle time of the linear part of the curve was designated Ct. Each sample was analyzed in duplicate and normalized to GAPDH using the equation $\Delta Ct_{SLC30A2} = Ct_{SLC30A2} - Ct_{GAPDH}$. The fold change in the SLC30A2 expression of cells transfected with SLC30A2-specific siRNA relative to control siRNA was calculated using the following equation: $2^{(\Delta\Delta CtSLC30A2)}$, where $\Delta\Delta Ct_{SLC30A2}$ = mean $\Delta Ct_{SLC30A2}$ of control − mean $\Delta Ct_{SLC30A2}$ of SLC30A2-specific knockdown. Values represent mean fold change ± S.D., relative to control (set to 100%).

RESULTS

Infants of subjects II:8 and III:3 (Fig. 1) were both delivered at term and exclusively breast-fed for five months. Both infants (subjects III:8 and IV:1) developed severe zinc deficiency (serum zinc concentration in infant III:8, 0.66 mg of zinc/liter at 24 weeks of age; normal range, 0.82 ± 0.03 mg of zinc/liter) (19). Individuals II:8 and III:3 had low milk zinc concentration (II:8, 0.26 mg of zinc/liter, week 24 of lactation; III:3, 0.23 mg zinc/liter, week 15 of lactation; normal range, 1.0–1.5 mg of zinc/liter at 3–6 months of lactation (20); however, serum zinc concentration in these women was normal (II:8, 1.0 mg of zinc/liter). Prior to zinc supplementation, alopecia and severe dermatitis were visible on the head, back, face (Fig. 2, *A–C*), and perigenital area (not shown) of infant III:8. Infant IV:1 presented with similar rashes starting at three months of age (images not shown). Dermatitis improved significantly in both affected infants within one week following the initiation of zinc supplementation (Fig. 2*D*), and the cessation of zinc supplementation following weaning did not lead to a relapse of zinc deficiency in either infant, excluding AE as a possible diagnosis. No consistent or remarkable symptoms other than neonatal zinc deficiency were reported in any other family member. These symptoms and clinical data are consistent with other reported cases of transient neonatal zinc deficiency due to low milk zinc concentration in exclusively breast-fed infants.

Similar to the findings of Michalczyk *et al.* (7), we found no mutations predicted to affect protein expression or function in SLC30A4 nor did we find any mutations in SLC39A3. However, sequence analysis of SLC30A2 in the two affected women (II:8 and III:3) determined that they were heterozygous for a missense mutation in exon 2 of SLC30A2, which substituted an adenine for guanine (Ade→Gua) and resulted in a change of histidine to arginine at amino acid position 54 (H54R) (Fig. 3*A*). Subsequent genomic analysis of subjects II:2 and II:6 identified them as heterozygotes as well, whereas subject II:4 was not examined, as she did not nurse her child, thus eliminating the possibility of examining her phenotype. The H54R mutation resides in a histidine-rich region conserved across human, mouse, and rat SLC30A2 and human and mouse SLC30A3 and SLC30A8 (Fig. 3*B*) and is not present in either the NCBI single nucleotide polymorphisms or expressed sequence tag data bases (data not shown). Topology prediction of ZnT-2 using the

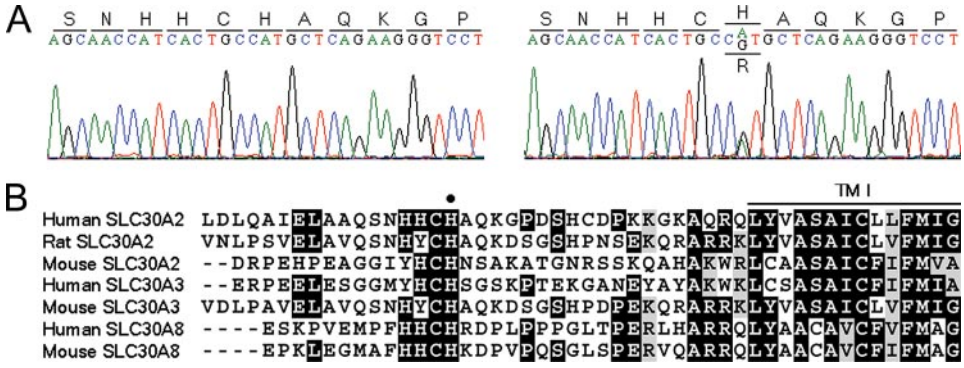

FIGURE 3. **Identification of a mutation in SLC30A2 in subjects with low zinc concentration and amino acid alignment of related proteins.** Shown are DNA chromatograms of control (*A*, *left*) and the representative affected individual (*A*, *right*). The affected subject is heterozygous for an adenine to guanine substitution, which replaces histidine (*H*) with arginine (*R*) at amino acid 54. The amino acid alignment (*B*) between human, rat, and mouse SLC30A2 and human and mouse SLC30A3 and SLC30A8 was generated with ClustalW and Boxshade. The mutation is located in a conserved region (marked with a *filled circle*) before the first predicted transmembrane domain (*TM I*, marked with a *bold line* above amino acid sequence).

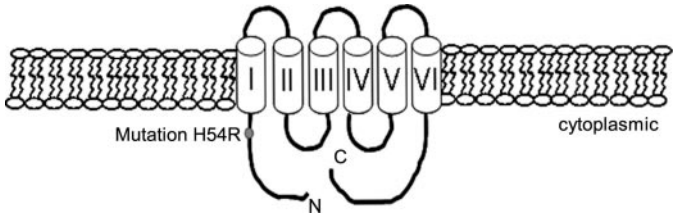

FIGURE 4. **Predicted topology of ZnT-2 indicating the location of the H54R mutation.** A model of ZnT-2 membrane topology illustrating the six transmembrane domains, intracellular N and C termini, and the location of the H54R substitution (marked with a *filled circle*) identified in subjects with low milk zinc concentration.

proteomic base server TopPred (21) predicts that this mutation resides within the N-terminal region immediately upstream from the first transmembrane domain and is localized intracellularly (Fig. 4).

Identification of a mutation in ZnT-2 first required determination of the role of ZnT-2 in mammary epithelial cell zinc transport. Toward this end, HC11 cells were transiently transfected with SLC30A2-specific siRNA, which successfully reduced ZnT-2 mRNA and protein expression (Fig. 5, *A* and *B*) and resulted in decreased zinc efflux (Fig. 5*C*). No difference was observed in zinc uptake due to SLC30A2 knockdown (Fig. 5*D*), indicating that ZnT-2 mediates zinc secretion from the mammary epithelial cell and that abrogation of zinc secretion following ZnT-2 knockdown is not due to impaired zinc uptake.

To determine the effects of the H54R mutation on zinc secretion, HEK-293 cells were transfected with empty pcDNA3.1 plasmid or plasmid containing wild-type or mutant SLC30A2. HEK-293 cells transfected with wild-type SLC30A2 secreted ~30% more zinc relative to cells transfected with empty plasmid and cells transfected with the H54R mutant SLC30A2 (Fig. 6). There was no difference in zinc uptake (data not shown) in cells transfected with either wild-type or mutant SLC30A2 compared with cells transfected with empty plasmid, indicating that increased zinc secretion in cells transfected with wild-type SLC30A2 is not due to increased zinc uptake. To determine whether expression of the mutant allele is a dominant negative mutation that impairs expression or function of wild-type ZnT-2 protein, HEK-293 cells were co-transfected with plasmids containing the wild-type and H54R mutant SLC30A2, and effects on zinc secretion were determined. Our data document that co-expression of wild-type and H54R mutant ZnT-2 did not abrogate increased zinc secretion observed in cells overexpressing wild-type ZnT-2 alone (Fig. 7) and suggest that decreased zinc secretion associated with the H54R mutant form of ZnT-2 does not result from a dominant negative interaction.

To determine the mechanisms through which the H54R mutation interferes with zinc secretion, effects on ZnT-2 protein abundance and subcellular localization were determined. HEK-293 cells were transfected with plasmid containing wild-type or mutant SLC30A2 fused to HA, and the resultant ZnT-2 protein was characterized by immunoblotting. Data indicate that cells transfected with either wild-type or H54R mutant SLC30A2 resulted in the translation of ZnT-2 protein with a molecular mass of ~48 kDa, which corresponds to the predicted molecular mass of ZnT-2 (Fig. 8*A*). Immunoblotting of the resulting supernatant from cell lysates centrifuged at 2,000 × *g* (slow sedimentation) indicated that, in HEK-293 cells transfected with equal amounts of plasmid, only ~33% of the H54R mutant protein was detected as compared with the wild-type protein, suggesting that the H54R mutation decreased ZnT-2 protein stability, increased degradation, or resulted in the trapping of mutant ZnT-2 protein in large molecular weight aggregates. We first verified that the reduced abundance of the H54R mutant was not due to transfection efficiency or cytotoxicity, as there was no difference in the amount of β-galactosidase detected in cells co-transfected with β-galactosidase. To further characterize the effects of the H54R mutation on ZnT-2 protein abundance, cells lysates from HEK-293 cells transfected with equal amounts of wild-type or H54R mutant plasmid were centrifuged at 800 × *g* to pellet only cellular debris and nuclei. Immunoblotting of post-nuclear lysates using both anti-HA and anti-ZnT-2 antibody documented a similar abundance of wild-type and mutant ZnT-2 protein (Fig. 8*B*). Taken together, these data indicate that the H54R mutant form of ZnT-2 was likely trapped in large molecular weight aggregates, as has been observed for other mistranslated proteins (22).

To investigate the possibility of aggresomal accumulation, we used confocal microscopy and determined that, in contrast to the diffuse vesicular staining observed for wild-type ZnT-2 (Fig. 9, *A*–*C*), the distribution of the H54R mutant form of ZnT-2 was restricted and localized to a distinct, large perinuclear compartment (Fig. 9, *D*–*F*). To complement the visual identification of aggresomal localization of the H54R mutant form of ZnT-2, we then utilized a cellulose acetate filter retardation assay (23) and documented that, although minimal ZnT-2 from HEK-293 cells overexpressing wild-type SLC30A2 was detected in aggresomes, a large abundance of the H54R mutant was trapped as detergent-insolu-

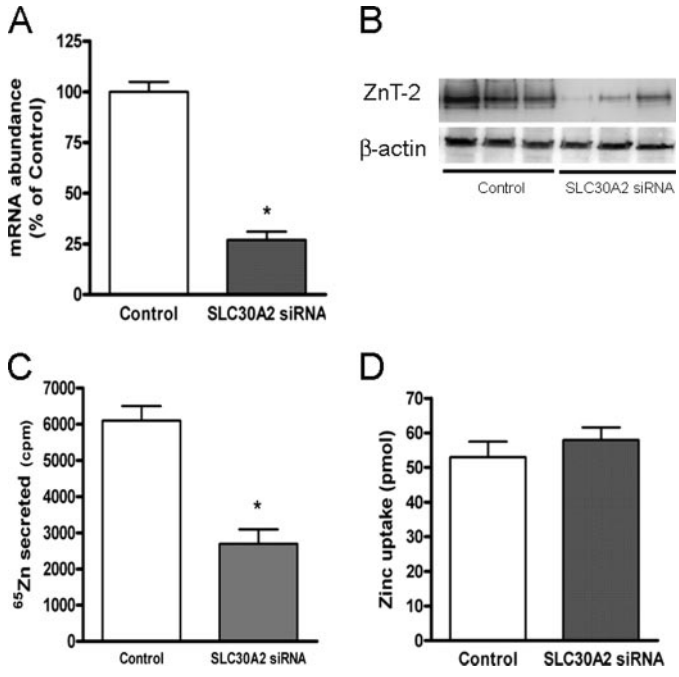

FIGURE 5. **ZnT-2 mRNA and protein abundance and zinc secretion is reduced in HC11 cells transfected with SLC30A2-specific siRNA.** SLC30A2 mRNA abundance (*A*) is expressed relative to GAPDH expression, and values represent percentage (mean ± S.D., $n = 5$) relative to control (set to 100%). Shown is a representative immunoblot of ZnT-2 protein (*B*) in cells transfected with control or SLC30A2-specific siRNA, ($n = 3$ samples/treatment). Equal sample loading was verified by reprobing for β-actin. Zinc secretion (*C*) was measured over 30 min after pretreatment with ^{65}Zn for 2.5 h, whereas zinc uptake (*D*) was measured over 30 min with ^{65}Zn. Values represent ^{65}Zn quantified (secretion, mean counts/min ± S.D.; $n = 6$) and pmol zinc (uptake, mean ± S.D.; $n = 6$). *Asterisk* indicates significant effect of SLC30A2 knockdown as analyzed by Student's *t* test ($p < 0.05$).

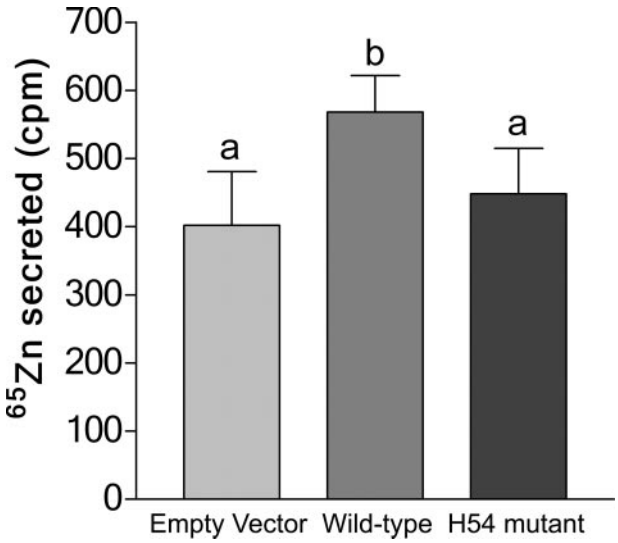

FIGURE 6. **Zinc secretion is reduced in HEK-293 cells expressing the H54R mutant form of ZnT-2.** Cells were preincubated in serum-free medium containing 0.1 μM $ZnCl_2$ and 0.1 μCi ^{65}Zn for 3 h. Medium was replaced, and ^{65}Zn secretion was measured over 30 min. Values represent ^{65}Zn quantified (mean counts/min ± S.D., $n = 4$ from three independent experiments). Means with different letters are significantly different as analyzed by one-way analysis of variance followed by a Tukey post-test ($p < 0.05$).

ble aggregates (Fig. 10). Taken together, these data suggest that the Ade→Gua substitution in SLC30A2 ultimately results in abrogated zinc secretion due to decreased abundance of functional ZnT-2 protein as a consequence of subcellular aggregation of the mutant form of ZnT-2, most likely due to protein misfolding.

DISCUSSION

The results from this study highlight the interdependence between genetics and nutrition, a concept which is just beginning to be appreciated. Although zinc deficiency is believed to result primarily from low dietary zinc intake or impaired zinc bioavailability, two genetic disorders in mammalian zinc metabolism that result in severe zinc deficiency have previously been identified. However, results from this study and others (7) indicate that neither of these genetic abnormalities are responsible for transient neonatal zinc deficiency in humans. Recent advances in the identification and characterization of tissue- and cell-specific zinc transporters (24, 25) now afford us the opportunity to examine this interplay in much greater detail and will further our understanding of the complex regulation of zinc metabolism and effects of nutrition on this process. Illustration of this interdependence is demonstrated in this study by the severity of zinc deficiency in two infants afflicted by transient neonatal zinc deficiency as a consequence of reduced zinc secretion into the milk of their nursing mothers, which we have determined results from a genetic defect in the gene encoding the zinc transporter ZnT-2 substituting a histidine for an arginine at amino acid residue 54. Left untreated, this condition can retard growth, impair immune function, and can even lead to death (1). The complexity of this disorder is compounded by the fact that, although the genotype and low milk zinc concentration phenotype is present in the mother, the symptomatic presentation of this disorder exists in her exclusively nursed infant, and thus the genetic defect may go unrecognized because of the lack of maternal symptoms or may be masked due to intake of zinc-containing food by the infant.

As is typical in this disorder, determining the pattern of inheritance and penetrance is extraordinarily difficult, primarily as a consequence of identifying the phenotype of low milk zinc concentration. The inheritance and penetrance of this disorder remains ambiguous in this family, because individual I:2 did not breast-feed her infants at all, and although individuals II:2 and II:6 are heterozygous for the H54R mutation, it was unclear as to whether they had the phenotypic reduction in mammary gland zinc secretion. Although the children of II:2 were breast-fed to 10–11 months of age and their mother recalled on questionnaires that both developed "diaper rash" at 8 weeks of age that did not respond to over-the-counter medication, which continued until weaning (suggesting presentation of the low milk zinc phenotype), both were fed infant formula (containing >5 mg of zinc/liter) once a week starting at 1 and 8 weeks of age. Although also heterozygous for the H54R mutation, individual II:6 reported breast-feeding all three children without any symptoms of dermatitis or zinc deficiency; however, analysis of feeding records show that she also supplemented breast-feeding with infant formula starting three weeks after birth. Thus, in the absence of maternal and infant zinc status assessment and measurement of milk zinc concentration, the phenotype of individuals II:2 and II:6 may have been masked because of the high zinc intake of their infants from

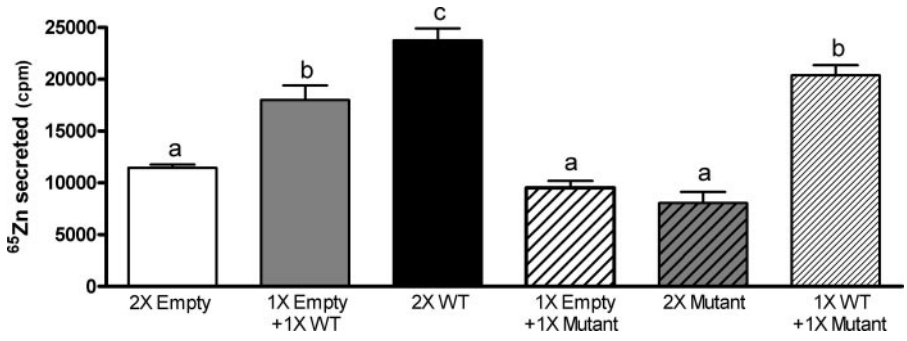

FIGURE 7. **Zinc secretion is not abrogated in HEK-293 cells co-expressing the H54R mutant and wild-type ZnT-2.** Cells were transfected with non-ligated pcDNA3.1 plasmid (1.6 μg; 2× empty), plasmid containing wild-type SLC30A2 (1.6 μg; 2× *WT*), or plasmid containing mutant SLC30A2 (1.6 μg; 2× mutant) or co-transfected with a combination of non-ligated plasmid and plasmid containing wild-type SLC30A2 (0.8 μg of each; 1× empty + 1× *WT*), non-ligated plasmid and plasmid containing mutant SLC30A2 (0.8 μg of each; 1× empty + 1× mutant), or plasmids containing wild-type and mutant SLC30A2 (0.8 μg of each; 1× WT + 1× mutant). Cells were preincubated in serum-free medium containing 0.1 μM $ZnCl_2$ and 0.1 μCi ^{65}Zn for 3 h. Medium was replaced and ^{65}Zn secretion (*A*) was measured over 30 min. Values represent ^{65}Zn secreted into medium (mean counts/min ± S.D., $n = 6$ from two independent experiments). Means with different letters are significantly different as analyzed by one-way analysis of variance followed by a Tukey post-test ($p < 0.05$).

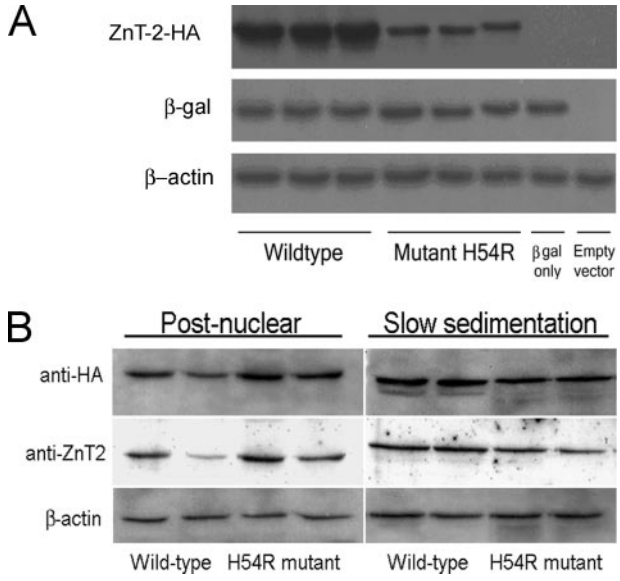

FIGURE 8. **Protein abundance of wild-type and H54R mutant ZnT-2 in transfected HEK-293 cells.** *A*, representative immunoblot of cell lysates (30 μg of protein/lane) following slow speed sedimentation of HEK-293 cells transfected with empty plasmid or cells expressing wild-type or the H54R mutant form of ZnT-2 and β-galactosidase and then detected with anti-HA, anti-β-galactosidase, or anti-β-actin antibody. The molecular mass of the transfected ZnT-2 protein is ~48 kDa. *B*, representative immunoblot of post-nuclear cell lysates and cell lysates following slow speed sedimentation (30 μg of protein/lane) of HEK-293 cells expressing wild-type or the H54R mutant form of ZnT-2 detected with anti-HA and then reprobed using affinity-purified anti-ZnT-2 and β-actin antibody.

formula, and further studies in other affected cohorts will be needed to establish the penetrance of this mutation. Nonetheless, as the condition was confirmed in both II:8 and III:3, the assumption of a Mendelian pattern of inheritance (barring sex linkage and assuming complete penetrance) suggests that either the condition has a dominant pattern of inheritance or individual II:1 is a carrier in the case of recessive transmission. Another study of transient neonatal zinc deficiency (18) supports the possibility of dominant inheritance, because in one family, three of four related sisters had low breast milk zinc concentration, and their infants developed transient neonatal zinc deficiency. Studies are currently underway to determine the incidence and inheritance pattern of this mutation in humans.

Although previous studies have shown that Zip3 and ZnT-4 have significant roles in mammary gland zinc transport (11, 26), we were unable to find any evidence of mutation in either SLC39A3 (Zip3) or SLC30A4 (ZnT-4) in any members of the afflicted family, similar to a previous report from Michalczyk *et al.* (7) in two unrelated individuals with low milk zinc concentration. As a result, we expanded our search to include SLC30A2, which encodes ZnT-2, a zinc transporter whose expression, although somewhat restricted, has been detected in the mammary gland (15). The identification of a mutation in ZnT-2 first required further clarification of the role of ZnT-2 in mammary epithelial cell zinc transport, because although ZnT-2 protein abundance is highest during early lactation and it is localized proximal to the luminal membrane rat mammary gland (suggesting a role in mammary epithelial cell zinc secretion) (15), it has been previously characterized to be localized to endosomes or lysosomes in transfected cell models (27). We verified the role of endogenous ZnT-2 in zinc secretion using siRNA-mediated knockdown of SLC30A2 expression in mammary epithelial cells, illustrating that zinc secretion was significantly reduced. It should be noted that zinc secretion was not completely abolished in cells treated by siRNA-mediated knockdown of SLC30A2, despite the significant reduction in ZnT-2 mRNA and protein expression. Although this may simply reflect residual ZnT-2 expression, it may also suggest that more than one zinc transporter participates in zinc secretion into milk. Similarly, in the lethal milk mouse, milk zinc concentration is reduced by ~50% (28), which suggests that some residual milk zinc secretion still occurs despite the truncation mutation in SLC30A4. Huang and Gitschier (11) hypothesize the possible existence of an additional mammary gland zinc transport pathway. Precedence for zinc transporter redundancy and even interaction exists, as disruption of both SLC30A5 (ZnT-5) and SLC30A7 (ZnT-7) in the chicken DT40 B cell line results in a greater reduction in the activity of the zinc-dependent enzyme alkaline phosphatase than disruption of either gene alone (29). This demonstrates that more than one zinc transporter contributes toward the delivery of zinc to alkaline phosphatase, lending credence to the possibility that ZnT-2 may interact with additional zinc transport proteins or processes and that not a single transporter may account for the entirety of mammary gland zinc secretion.

Identification of the Ade→Gua mis-sense mutation in SLC30A2 in the affected subjects suggests that the H54R substitution has a significant impact on ZnT-2 function, and in fact, we determined that expression of the mutated form of ZnT-2 resulted in decreased zinc secretion from transfected

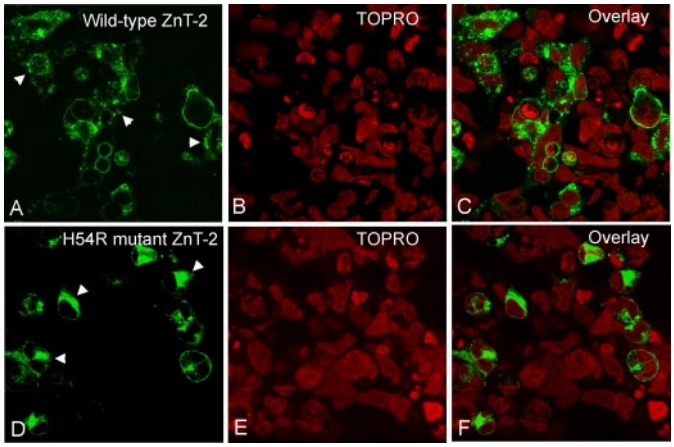

FIGURE 9. **Subcellular localization of the H54R mutant form of ZnT-2 suggests aggresomal accumulation.** Localization of wild-type (*A–C*) or the H54R mutant (*D–F*) ZnT-2 fused to an HA tag in transfected HEK-293 cells was examined using confocal microscopy. ZnT-2 was detected with Alexa 488-conjugated anti-HA antibody (*green*; *A* and *D*), and the nucleus was stained with TOPRO nucleic acid dye (*red*; *B* and *E*). *Overlay images* illustrate vesicular localization of wild-type (*C*) or perinuclear clustering of the H54R mutant form (*F*) of ZnT-2. Magnification of 100× under oil.

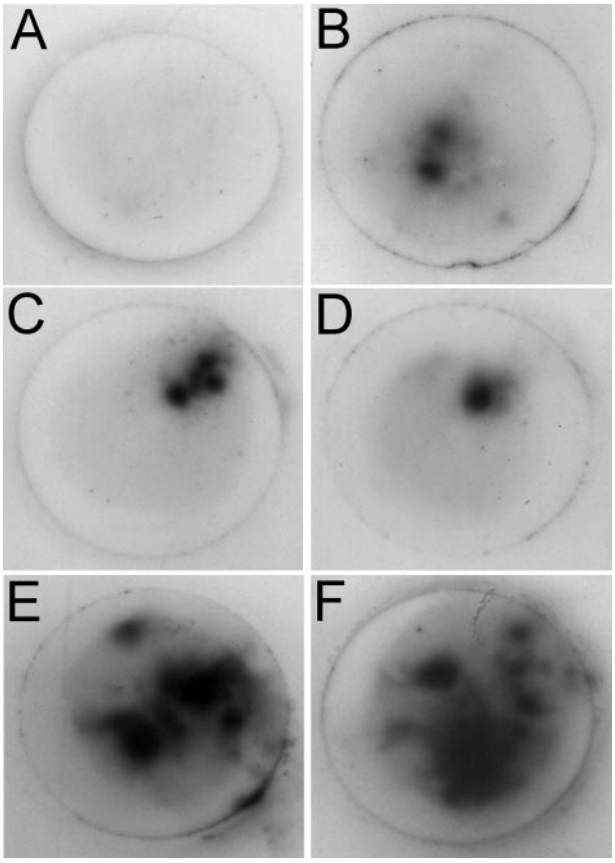

FIGURE 10. **Identification of the H54R mutant form of ZnT-2 in detergent-insoluble aggresomes by immunoblotting.** Detergent-insoluble proteins (100 μg of total cell protein/filter) were trapped by vacuum filtration. Representative immunoblots of cellulose acetate filters of cell lysates from HEK-293 cells transfected with empty vector (*A* and *B*) or cells expressing wild-type (*C* and *D*) or H54R mutant (*E* and *F*) ZnT-2 fused to an HA tag detected with anti-HA antibody (0.5 μg/ml) and visualized using chemiluminescence.

HEK-293 cells. Heterozygous mutations can often result in phenotypic presentation as a consequence of either haploinsufficiency or dominant negative effects exerted by the mutant protein; however, the lack of effect from co-expression of the H54R mutant and wild-type ZnT-2 on zinc secretion suggests that effects of this mutation are more subtle. One possibility is that the H54R mutation results in the loss of a histidine residue that is critical for protein function. The H54R mutation is located in a region with well conserved histidine and cysteine residues, and both amino acids are known to participate as metal binding sites. For example, a similar His→Arg substitution in SOD1 (superoxide dismutase 1) disrupts its copper binding site (30) and is associated with the genetic disorder familial amyotrophic lateral sclerosis (31). Huang and Gitschier (11) further speculate that the N-terminal domain of ZnT-4 plays an integral role in zinc binding, although through different amino acid residues. However, the role of these different residues (histidine, cysteine, or aspartate) in the zinc transporting function of zinc transporters has not been characterized, and further *in vitro* studies will be required to determine the effects of this mutation on the metal binding and transporting properties of ZnT-2.

Alternatively, the His→Arg substitution may alter ZnT-2 protein conformation, possibly as a result of the difference in isoelectric points between arginine (11.15) and histidine (7.47). Ionic interactions between amino acids may affect protein stability through repulsion and attraction properties, and the net contribution of these interactions governs protein folding and stability. The appearance of mutant ZnT-2 aggregation, which we detected by both confocal microscopy and detergent-insoluble filtration, is characteristic of protein misfolding (32) and is similar to observations made in tissue samples from patients with a similar His→Arg mutation in SOD1 (33), suggesting that the His→Arg substitution in ZnT-2 results in protein misfolding and targets the misfolded protein for degradation. Although accumulation of proteinaceous inclusions often results in cytotoxity (34), this was not observed in HEK-293 cells expressing the H54R mutated form of ZnT-2, suggesting limited effects of this mutation on overall cellular function and perhaps explaining the lack of clinical symptoms in afflicted women.

In summary, our findings reveal that ZnT-2 plays a major role in mammary epithelial cell zinc secretion and suggest that a mutation in this gene may be responsible for low milk zinc concentration and transient neonatal zinc deficiency in humans. This study also supports the hypothesis by Michalczyk *et al.* (7) that the genetic mutation responsible for transient neonatal zinc deficiency in humans is not the same as that identified in the lethal milk mouse. The lack of association between maternal zinc status and breast milk zinc concentration (20) combined with the genetic etiology of low breast milk zinc levels also suggests that non-dietary factors, such as genetic mutations or polymorphisms, may underlie the large interindividual variability observed in milk zinc concentration (20), illustrating the interplay between genes and nutrition.

Acknowledgments—We thank family members for their interest and cooperation in this study and Jose Ignacio Gonzales Zambra for excellent technical assistance. The ABI 7900 real-time thermocycler was funded by a grant to the University of California, Davis, Clinical Nutrition Research Unit (NIH DK35747).

REFERENCES

1. Aggett, P. J., and Harries, J. T. (1979) *Arch. Dis. Child.* **54,** 909–917
2. Krebs, N. F. (2000) *J. Nutr.* **130,** (suppl.) 358S–360S
3. Aggett, P. J., Atherton, D. J., More, J., Davey, J., Delves, H. T., and Harries, J. T. (1980) *Arch. Dis. Child.* **55,** 547–550
4. Parker, P. H., Helinek, G. L., Meneely, R. L., Stroop, S., Ghishan, F. K., and Greene, H. L. (1982) *Am. J. Dis. Child.* **136,** 77–78
5. Weymouth, R. D., Kelly, R., and Lansdell, B. J. (1982) *Aust. Paediatr. J.* **18,** 208–210
6. Atkinson, S. A., Whelan, D., Whyte, R. K., and Lönnerdal, B. (1989) *Am. J. Dis. Child.* **143,** 608–611
7. Michalczyk, A., Varigos, G., Catto-Smith, A., Blomeley, R. C., and Ackland, M. L. (2003) *Hum. Genet.* **113,** 202–210
8. Atherton, D. J., Muller, D. P., Aggett, P. J., and Harries, J. T. (1979) *Clin. Sci.* (*Lond.*) **56,** 505–507
9. Wang, K., Zhou, B., Kuo, Y. M., Zemansky, J., and Gitschier, J. (2002) *Am. J. Hum. Genet.* **71,** 66–73
10. Kury, S., Dreno, B., Bezieau, S., Giraudet, S., Kharfi, M., Kamoun, R., and Moisan, J. P. (2002) *Nat. Genet.* **31,** 239–240
11. Huang, L., and Gitschier, J. (1997) *Nat. Genet.* **17,** 292–297
12. Piletz, J. E., and Ganschow, R. E. (1978) *Science* **199,** 181–183
13. Sandström, B., Cederblad, Å., Lindblad, B. S., and Lönnerdal, B. (1994) *Arch. Pediatr. Adolesc. Med.* **148,** 980–985
14. Erway, L. C., and Grider, A. Jr. (1984) *J. Hered.* **75,** 480–484
15. Kelleher, S. L., and Lönnerdal, B. (2003) *J. Nutr.* **133,** 3378–3385
16. Hall, T. A. (1999) *Nucleic Acids Symp. Ser.* **41,** 95–98
17. Kelleher, S. L., and Lönnerdal, B. (2002) *J. Nutr.* **132,** 3280–3285
18. Matsumoto, G., Stojanovic, A., Holmberg, C. I., Kim, S., and Morimoto, R. I. (2005) *J. Cell Biol.* **171,** 75–85
19. Kasperek, K., Feinendegen, L. E., Lombeck, I., and Bremer, H. J. (1977) *Eur. J. Pediatr.* **126,** 199–202
20. Krebs, N. F., Reidinger, C. J., Hartley, S., Robertson, A. D., and Hambidge, K. M. (1995) *Am. J. Clin. Nutr.* **61,** 1030–1036
21. Claros, M. G., and von Heijne, G. (1994) *Comput. Appl. Biosci.* **10,** 685–686
22. Bross, P., Corydon, T. J., Andresen, B. S., Jorgensen, M. M., Bolund, L., and Gregersen, N. (1999) *Hum. Mutat.* **14,** 186–198
23. Wanker, E. E., Scherzinger, E., Heiser, V., Sittler, A., Eickhoff, H., and Lehrach, H. (1999) *Methods Enzymol.* **309,** 375–386
24. Palmiter, R. D., and Huang, L. (2004) *Pfluegers Arch.* **447,** 744–751
25. Eide, D. J. (2004) *Pfluegers Arch.* **447,** 796–800
26. Kelleher, S. L., and Lönnerdal, B. (2005) *Am. J. Physiol.* **288,** C1042–C1047
27. Palmiter, R. D., Cole, T. B., and Findley, S. D. (1996) *EMBO J.* **15,** 1784–1791
28. Ackland, M. L., and Mercer, J. F. (1992) *J. Nutr.* **122,** 1214–1218
29. Suzuki, T., Ishihara, K., Migaki, H., Matsuura, W., Kohda, A., Okumura, K., Nagao, M., Yamaguchi-Iwai, Y., and Kambe, T. (2005) *J. Biol. Chem.* **280,** 637–643
30. Liu, H., Zhu, H., Eggers, D. K., Nersissian, A. M., Faull, K. F., Goto, J. J., Ai, J., Sanders-Loehr, J., Gralla, E. B., and Valentine, J. S. (2000) *Biochemistry* **39,** 8125–8132
31. Aoki, M., Ogasawara, M., Matsubara, Y., Narisawa, K., Nakamura, S., Itoyama, Y., and Abe, K. (1994) *J. Neurol. Sci.* **126,** 77–83
32. Johnston, J. A., Ward, C. L., and Kopito, R. R. (1998) *J. Cell Biol.* **143,** 1883–1898
33. Shibata, N., Asayama, K., Hirano, A., and Kobayashi, M. (1996) *Dev. Neurosci.* **18,** 492–498
34. Bruijn, L. I., Miller, T. M., and Cleveland, D. W. (2004) *Annu. Rev. Neurosci.* **27,** 723–749